



Geogenic particles induce bronchial susceptibility to non-typeable *Haemophilus influenzae*

Lewis J. Williams^a, Stephen G. Tristram^b, Graeme R. Zosky^{a,c,*}

^a Tasmanian School of Medicine, University of Tasmania, Hobart, 7000, Australia

^b School of Health Sciences, University of Tasmania, Launceston, 7250, Australia

^c Menzies Institute for Medical Research, University of Tasmania, Hobart, 7000, Australia

ARTICLE INFO

Handling Editor: Jose L Domingo

Keywords:

Geogenic PM

Particulate matter

Iron oxide

Bronchiectasis

Non-typeable *Haemophilus influenzae* (NTHi)

ABSTRACT

Exposure to geogenic (earth-derived) particulate matter (PM) is linked to an increased prevalence of bronchiectasis and other respiratory infections in Australian Indigenous communities. Experimental studies have shown that the concentration of iron in geogenic PM is associated with the magnitude of respiratory health effects, however, the mechanism is unclear. We investigated the effect of geogenic PM and iron oxide on the invasiveness of non-typeable *Haemophilus influenzae* (NTHi). Peripheral blood mononuclear cell-derived macrophages or epithelial cell lines (A549 & BEAS-2B) were exposed to whole geogenic PM, their primary constituents (haematite, magnetite or silica) or diesel exhaust particles (DEP). The uptake of bacteria was quantified by flow cytometry and whole genome sequencing (WGS) was performed on NTHi strains. Geogenic PM increased the invasiveness of NTHi in bronchial epithelial cells. Of the primary constituents, haematite also increased NTHi invasion with magnetite and silica having significantly less impact. Furthermore, we observed varying levels of invasiveness amongst NTHi isolates. WGS analysis suggested isolates with more genes associated with heme acquisition were more virulent in BEAS-2B cells. The present study suggests that geogenic particles can increase the susceptibility of bronchial epithelial cells to select bacterial pathogens *in vitro*, a response primarily driven by haematite content in the dust. This demonstrates a potential mechanism linking exposure to iron-laden geogenic PM and high rates of chronic respiratory infections in remote communities in arid environments.

1. Introduction

Indigenous Australians are disproportionately affected by respiratory tract infections. Compared to the non-Indigenous population, Indigenous Australians have a 7-fold greater hospitalisation rate for respiratory infections (Pak et al., 2021). Following this, 1–2% of Indigenous children are diagnosed with bronchitis and suffer from some of the highest rates of non-cystic fibrosis bronchiectasis globally (Chang et al., 2002). Overall, rates of bronchiectasis amongst Indigenous communities are three times higher than in other parts of the country with disease onset occurring far earlier in life compared to non-Indigenous bronchiectasis patients (Blackall et al., 2018).

Up to 90% of Indigenous Australians with bronchiectasis test positive for pathogenic bacteria, predominantly non-typeable *Haemophilus influenzae* (NTHi) (Angrill et al., 2002; Blackall et al., 2018; Pinto et al., 2016; Pizzutto et al., 2017; Watson et al., 2006). Factors contributing to higher rates of bacterial infection in Indigenous populations include

poor nutrition and housing, high rates of smoking, lower socio-economic status, and poor access to health care (Australian Bureau of Statistics, 2017; Melody et al., 2016; O'Grady et al., 2010). However, there are other external factors that may be contributing to this issue. For example, there is evidence suggesting that traffic-derived pollutants such as diesel exhaust particulates (DEP) can exacerbate airway infection (Castranova et al., 2001; Siegel et al., 2004; Yang et al., 2001) and more recent evidence suggests that geogenic (earth-derived) particulates can also increase the risk and severity of bacterial respiratory infections (Government of South Australia, 2007; Government of Western Australia, 2016; Mullan et al., 2006). Exposure to the latter particles is a particular issue in remote Indigenous communities (Clifford et al., 2015) which may be contributing to the disproportionate disease burden. However, the mechanisms linking exposure to environmental particulates and an increased risk and severity of bacterial infections is largely unknown.

Potential mechanisms include an enhanced capacity of bacteria to

* Corresponding author. College of Health and Medicine, University of Tasmania, Hobart, 7000, Australia.

E-mail address: graeme.zosky@utas.edu.au (G.R. Zosky).

<https://doi.org/10.1016/j.envres.2023.116868>

Received 22 June 2023; Received in revised form 8 August 2023; Accepted 8 August 2023

Available online 9 August 2023

0013-9351/© 2023 The Author(s). Published by Elsevier Inc. This is an open access article under the CC BY-NC license (<http://creativecommons.org/licenses/by-nc/4.0/>).

invade lung cells (Shepherd et al., 2019) or an impairment in the innate immune response. Bacterial invasion in the lung primarily occurs in airway epithelial cells and provides protection from the host immune response, as well as antibiotics, enabling persistent infection (Clementi and Murphy, 2011; Esen et al., 2001; Foxwell et al., 1998). Lung macrophages are the first line of innate defence against inhaled pathogens through phagocytosis of bacteria and modulation of the subsequent immune response (Rubins, 2003). Given that macrophages also phagocytose particulates under 10 μM (Chikaura et al., 2016), and this size fraction includes geogenic particulates, it is possible that such exposure may impair macrophage function towards pathogens.

The aim of this study was to determine whether particulate matter (geogenic, inorganic or DEP) modifies the invasiveness of clinically relevant strains of NTHi in bronchial and alveolar epithelial cells and macrophages, as the primary cell types involved in the innate response to bacterial pathogens.

2. Methods

2.1. Cell culture

The transformed human bronchial epithelial cell line (BEAS-2B; ATCC CRL-9609) was cultured in 75 cm^2 flasks (Corning CLS3290), using serum-free bronchial epithelial growth medium (BEGM; Lonza CC-33170) at 37 °C in a humidified atmosphere of 5% CO_2 . Similarly, the alveolar epithelial cell line (A549; ATCC CCL-185) was cultured in F-12K medium (ATCC 30-2004) supplemented with 10% FBS under the same conditions.

Peripheral blood mononuclear cells (PBMCs) were isolated from six healthy adults aged between 20 and 50 years of age. Briefly, 32 mL of blood was collected from each patient using EDTA- BD Vacutainers (BD 366643). Samples were incubated at room temperature for 20 min with gentle mixing. Blood was aseptically layered onto 4 mL of Histopaque (Sigma-Aldrich 10771) in a 1:1 ratio before being centrifuged at 100 g for 30 min. Density gradient separation allowed the isolation of mononuclear cells which were then washed twice by centrifugation at 300g. Cells were resuspended in serum-free RPMI-1640 and seeded at a density of 3×10^6 cells/mL. Cells were incubated for 1 h at 37 °C in a humidified atmosphere of 5% CO_2 and then washed twice to remove non-adherent cells, providing pure monocyte cultures confirmed by microscopy. RPMI-1640 media containing 10% FBS was supplemented with 2 ng/mL of granulocyte-macrophage colony-stimulating factor (GM-CSF; PeproTech 300-03) for 12 days, refreshing every 3 days, to obtain monocyte-derived macrophages. All human work was approved by the Tasmanian Health and Medical Human Research Ethics Committee (H0016505) and conducted according to guidelines of the National Health and Medical Research Council (Australia).

2.2. Particle preparation

Two surface soil samples were collected from Kalgoorlie (30°45'45" S 121°27'24" E) and Newman (23°21'25" S 119°43'51" E) in Western Australia. The chemical properties of these particles have been previously reported (Table 1) (Zosky et al., 2014) and are similar to airborne particles in these regions (Ljung et al., 2011). Notably, the Kalgoorlie sample was 53.82% silicon and 18.99% iron, whereas the Newman sample was 47.42% silicon and 30.59% iron (Zosky et al., 2014). Alongside these, commercially available standard preparations of dry silica (SiO_2 ; NIST, 1878B), haematite (Fe_2O_3 ; Sigma-Aldrich 310050), magnetite (Fe_3O_4 ; Sigma-Aldrich 31006) and DEP (NIST 1650b) were used. All samples were exposed to UV light for 2 h, baked at 120 °C for 20 min, to remove spore-forming fungi, and washed three times to remove bacteria and endotoxin.

For particle exposure, epithelial cells were seeded at a concentration of 2×10^5 cells/mL and exposed to vehicle control (culture media) or 75 $\mu\text{g}/\text{mL}$ of each particle type, or as otherwise specified, for 24 h. PBMC-

Table 1

ICP-MS analysis of dust samples from the Western Australian towns of Newman and Kalgoorlie identifying primary constituents of soil samples. Adapted from Zosky et al. (2014).

	Newman	Kalgoorlie
MMAD (μm)	2.93	3.45
GSD	2.49	3.4
Si (mg.kg)	186,000	170,000
Al (mg.kg)	84,000	82,200
Fe (mg.kg)	120,000	60,000
Mn (mg.kg)	1600	860
Cr (mg.kg)	210	360
Zn (mg.kg)	100	85
Ni (mg.kg)	110	140
Cu (mg.kg)	97	47
Pb (mg.kg)	49	2100
Co (mg.kg)	52	24
As (mg.kg)	8	34
U (mg.kg)	1	0.91
Cd (mg.kg)	0.05	0.08
Endotoxin (ng/50 μL)	0.5	2.3

derived macrophages were seeded at 5×10^5 cells/mL and exposed to 50 $\mu\text{g}/\text{mL}$ of each particle type for 24 h as higher doses were cytotoxic. All epithelial cell experiments were replicated independently six times, with PBMC studies replicated three times, using fresh preparations of particle solutions and cell cultures to allow valid statistical comparisons between exposure groups.

2.3. Bacterial isolates and culture

Eight clinical pathogenic strains of NTHi isolated from patients were used. In initial experiments, four strains isolated from sputum were used (Ci8, Ci16, Ci34 & Ci43). The panel of NTHi used in subsequent experiments were chosen to represent a wider diversity of isolates from different regions including the oropharynx (NF3) and the ear (Ci37, L267 & L341). The isolates were identified by the original laboratories as described in previous studies (Bradbury et al., 2008, 2009; Witherden and Tristram, 2013). NTHi was cultured on chocolate agar at 37 °C and 5% CO_2 before being transferred to Brain Heart Infusion (BHI) for overnight culture. Bacterial suspensions were incubated at 37 °C rotating at 200 rpm.

Bacterial broth suspensions were standardised to an optical density (OD) of 0.6 at a wavelength of 600 nm. There were no differences in CFU/mL between NTHi isolates at 0.6 OD. From this, 1 mL of each bacterial suspension was centrifuged at 6000 g for 10 min before three washes in sterile-filtered phosphate-buffered saline (PBS). Bacteria were resuspended in a total of 1 mL of PBS each and fluorescently tagged with 1 μL CellTrace Far Red (ThermoFischer, C34564) for 20 min at room temperature in the absence of light. Bacteria were diluted to a 1:30 concentration before 30 μL of bacterial suspension was applied per well in a 96-well plate and incubated for 3 h at 37 °C and 5% CO_2 .

After bacterial exposures, samples were washed using PBS and exposed to their respective growth media supplemented with 200 $\mu\text{g}/\text{mL}$ of gentamicin to remove remaining extracellular bacteria. Samples were incubated for 4 h at 37 °C and 5% CO_2 . Following PBS washing, trypsin detached cell samples were made to a final volume of 200 $\mu\text{L}/\text{well}$ for flow cytometry.

2.4. Flow cytometry

Fluorescent staining of bacteria was analysed using a BD FACS CANTO II flow cytometer (BD Biosciences, USA). Data were analysed using FCS Express 6 (DeNovo Software, USA), using fluorescence minus one (FMO) controls to determine gating strategies. Compensation was performed using single colour-stained cells, and compensation matrices were calculated and applied. Cell populations were distinguished based

on forward scatter (FSC) height and width. Gating strategies mitigated the presence of any remaining extracellular bacteria, while intracellular bacteria were quantified using the median fluorescent intensity.

2.5. Whole genome sequencing (WGS)

Genome sequencing was conducted using the Miseq (Illumina, USA) on NTHi strains used in the cell invasion assays. Galaxy Australia was used for all genomic preparation and annotation. Briefly, reads were trimmed using Trimmomatic (Bolger et al., 2014) and assembled using SPAdes (Bankevich et al., 2012). Assembled genomes were annotated using Prokka (Seemann, 2014) and quality checked with Quast (Gurvich et al., 2013). Roary was used to generate core gene alignments (Page et al., 2015) and compared to the SwissProt protein database using NCBI BLAST + blastx (Altschul et al., 1997; Camacho et al., 2009; Cock et al., 2015). RStudio 1.2.5 was then used to categorise genomes by principal component analysis (PCA) which was used to assess the relationship between gene expression and NTHi invasion. Unique genes and their respective proteins were then isolated by cross comparison of bacterial isolates and grouped functionally using the STRING functional protein network (Szklarczyk et al., 2019).

2.6. Statistical analysis

Comparisons between groups were made using one- and two-way ANOVA. When significance was determined for the main factors by ANOVA, the Turkey post-hoc test was used to examine individual between-group differences. Where necessary, the data were log transformed to satisfy the assumptions of normal distribution of the error terms and homoscedasticity of the variance. Associations between continuous variables were analysed using linear regression. All data are presented as mean (SD) and values of $p < 0.05$ were considered

statistically significant. All statistical analyses were conducted using Prism (v9).

3. Results

3.1. The effects of geogenic particles on NTHi invasion

Initial proof of concept studies were conducted on bacterial isolates exclusively derived from sputum samples. For statistical analyses in these experiments, the Ci8 strain was used as an arbitrary reference point for comparison against other NTHi strains (Ci16, Ci34 and Ci43). PBMC-derived macrophages internalized NTHi strains Ci16, Ci34 ($p < 0.001$) and Ci43 ($p = 0.02$) less than Ci8 (Fig. 1A), demonstrating a strain-dependent effect. However, there was no effect of particle exposure ($p > 0.05$) on NTHi invasiveness in these cells.

Conversely, NTHi strains Ci16 and Ci43 invaded A549 epithelial cells significantly more than Ci8 ($p < 0.001$) showing strain-dependent differences in invasion (Fig. 1B). However, DEP was the only particle type to alter internalization in these cells, decreasing Ci16 ($p < 0.001$) and Ci43 invasion ($p = 0.04$).

In contrast to the other cell types, there were no differences in bacterial invasion at baseline in BEAS-2B cells (Fig. 1C; $p > 0.05$). However, when cells were exposed to dusts from Kalgoorlie, internalization of Ci16 and Ci34 increased compared to control ($p < 0.001$) and DEP ($p = 0.003$ & $p < 0.001$). Furthermore, Newman dust increased internalization of Ci16, Ci34 ($p < 0.001$) and Ci43 ($p = 0.003$) compared to control and DEP ($p < 0.001$ & $p = 0.009$).

3.2. The importance of iron oxide in geogenic-induced invasion

Our initial data suggested that bronchial epithelial cells may be more susceptible to geogenic particle-enhanced invasion. In addition, these

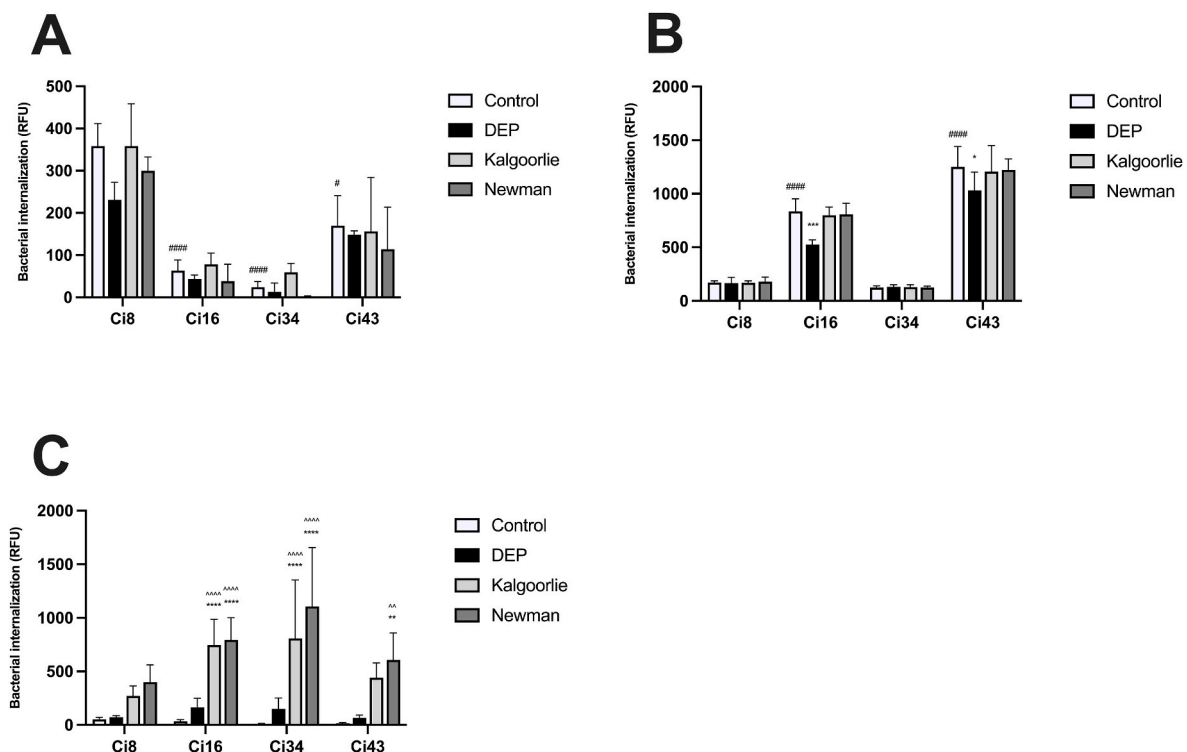


Fig. 1. NTHi internalization in (A) PBMC-derived macrophages exposed to 50 $\mu\text{g}/\text{mL}$ of particulates, (B) A549 epithelial cells and (C) BEAS-2B epithelial cells exposed to 75 $\mu\text{g}/\text{mL}$ of particulates for 24 h. Data are represented by median relative fluorescent units and presented as mean(SD) from 3 independent replicates for PBMCs and 6 independent replicates for epithelial cells, with # and #### indicating $p < 0.05$ and $p < 0.0001$ respectively versus Ci8 control, * and *** indicate $p < 0.05$ and $p < 0.001$ for the effect of exposure compared to control within each group and ^, ^^ and **** represent $p < 0.01$, $p < 0.001$ and $p < 0.0001$ compared to DEP.

data suggested that the effect was more pronounced in response to the Newman sample (Fig. 1C). Whilst both dust samples are very similar in the particle size, silicon and aluminium content, the Newman dusts contain twice as much iron (Table 1). Thus, we hypothesised that iron oxide is facilitating the invasion of NTHi, specifically in BEAS-2B cells. We compared the effects of environmental silicon (silica; SiO₂), to the most common environmental iron in Australia, haematite (Fe₂O₃), as well as a less common iron oxide, magnetite (Fe₃O₄), on NTHi invasion. Additionally, in order to determine whether the effects of these particles were limited to sputum isolates of NTHi, we included additional NTHi isolates from the oropharynx (NF3) and ear (Ci37, L267 & L341), whilst retaining two from the sputum experiments (Ci8 & Ci34). We exposed BEAS-2B, A549 cells and PBMC-derived macrophages to particles and NTHi to evaluate the role of iron oxide in the responses we observed.

PBMC-derived macrophages demonstrated differences in NTHi internalization consistent with the initial experiments (Fig. 2). NTHi Ci34 ($p = 0.002$), Ci37 ($p = 0.010$) and L267 ($p = 0.001$) were internalized significantly less than NF3, with no difference between NF3 and L341 but strain Ci8 ($p = 0.045$) was internalized more. As before, there was no effect of any particle exposure on the internalization of NTHi in PBMC-derived macrophages ($p > 0.05$).

Similarly, particles did not increase invasion in A549 alveolar epithelial cells (Fig. 3). With the additional NTHi strains, we demonstrate similar strain-dependent effects, with strains Ci34 ($p = 0.002$) and Ci37 ($p < 0.001$) being lower than NF3, whilst L267 and L341 were higher ($p < 0.001$). In contrast to the initial experiments on the sputum isolates we found effects in two of the highly invasive ear isolates with silica, magnetite and haematite reducing L267 internalization ($p < 0.001$), and haematite also reducing L341 internalization ($p = 0.028$).

Haematite significantly increased internalization of all NTHi strains compared to control and the other particle types in BEAS-2B cells (Fig. 4; $p < 0.001$). Silica induced a mixed, strain-dependent response. In strains NF3 and Ci8, it decreased internalization ($p < 0.001$), whereas in Ci34 and Ci37 it had no effect and it increased internalization in strains L267 and L341 ($p < 0.001$). Magnetite had a similar but lesser effect, decreasing NF3 internalization ($p < 0.001$) and increasing L267 ($p = 0.002$) internalization with no effect for any other strain ($p > 0.05$).

After identifying the importance of haematite in the bronchial epithelial cell response, we assessed the dose dependence of the response in a single NTHi strain (Ci43) (Fig. 5). Haematite significantly increased invasion, starting at 25 $\mu\text{g}/\text{mL}$ and continuing to 100 $\mu\text{g}/\text{mL}$ ($p < 0.001$). Dose-dependent increases occurred between 10 and 25 $\mu\text{g}/\text{mL}$ ($p = 0.001$) and 25 $\mu\text{g}/\text{mL}$ to 50 $\mu\text{g}/\text{mL}$ ($p < 0.001$), plateauing after 50 $\mu\text{g}/\text{mL}$ ($p < 0.05$).

3.3. Whole genome sequencing

In our functional studies, haematite increased the susceptibility of bronchial epithelial cells to NTHi invasion. However, we wanted to

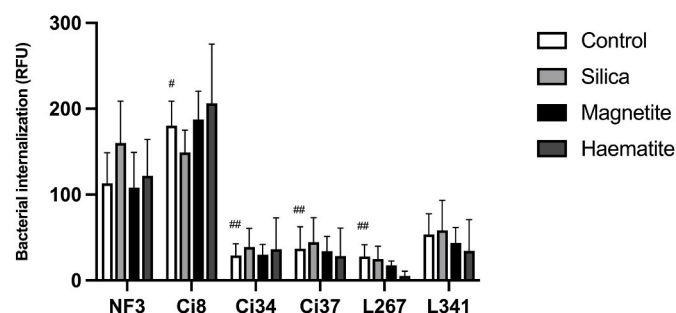


Fig. 2. NTHi internalization in PBMC-derived macrophages exposed to 50 $\mu\text{g}/\text{mL}$ of particulates for 24 h. Data are represented by median relative fluorescent units and presented as mean(SD) from 3 independent replicates with # and ## indicating $p < 0.05$ and $p < 0.01$ respectively versus NF3 control.

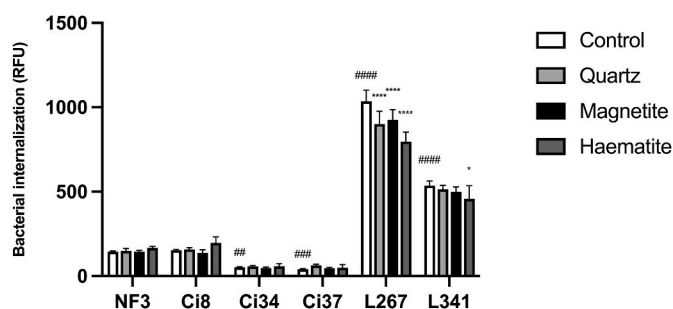


Fig. 3. NTHi internalization in A549 epithelial cells exposed to 75 $\mu\text{g}/\text{mL}$ of particulates for 24 h. Data are represented by median relative fluorescent units and presented as mean(SD) from 6 independent replicates with ##, ### and #### indicating $p < 0.01$, $p < 0.001$ and $p < 0.0001$ respectively versus NF3 control. * and **** indicate $p < 0.05$ and $p < 0.0001$ compared to control for each respective strain.

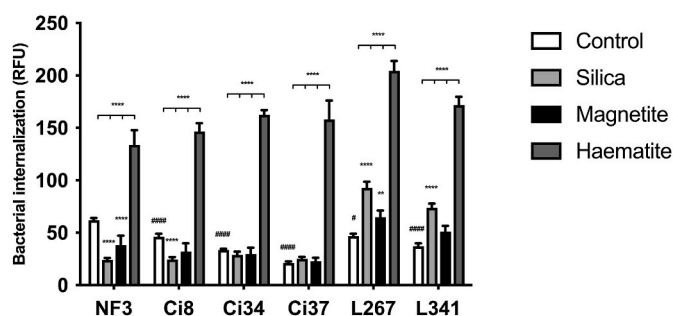


Fig. 4. NTHi internalization in BEAS-2B epithelial cells exposed to 75 $\mu\text{g}/\text{mL}$ of particulates for 24 h. Data are represented by median relative fluorescent units and presented as mean(SD) from 6 independent replicates with ## and #### indicating $p < 0.01$ and $p < 0.0001$ respectively versus NF3 control. * and **** indicate $p < 0.01$ and $p < 0.0001$ compared to control for each respective strain.

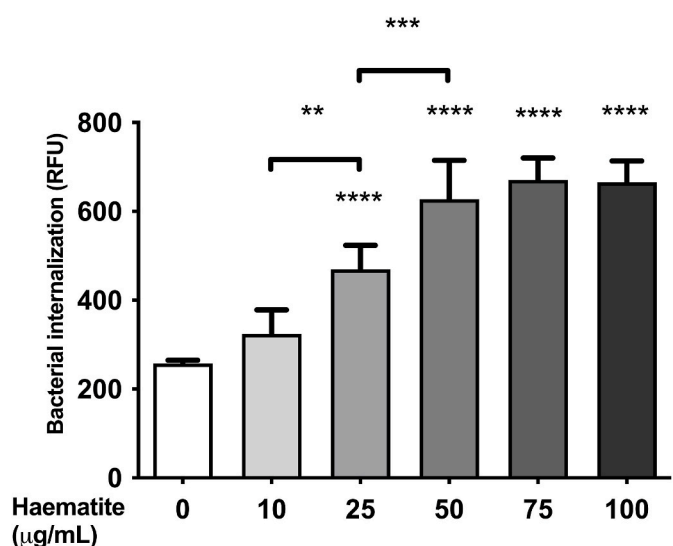


Fig. 5. NTHi strain Ci43 internalization in BEAS-2B epithelial cells exposed to haematite particulates for 24 h. Data are represented by median relative fluorescent units and presented as mean(SD) from 6 independent replicates with **, *** and **** indicating $p < 0.01$, $p < 0.001$ and $p < 0.0001$ respectively.

establish if there were genetic characteristics that may predispose to this response.

3.3.1. Principal component analysis (PCA)

Given the extent of the genomic data, PCA was used as a data reduction strategy for subsequent correlation with the significant NTHi invasion response to particles in BEAS-2B cells. Two principal components (PC1 and PC2) were identified that accounted for over 80% of the genomic variance. Significant associations were found between both PC1 and PC2 and the effect of silica, haematite ($p < 0.001$) and magnetite ($p = 0.001$) on NTHi invasion in BEAS-2B cells.

To identify the groups of genes that explained these associations, a filtering process was applied whereby clusters of isolates were qualitatively identified when the regression analysis was significant (Table 2), and the relationship was monotonic (Fig. 6). This filtration process isolated clusters of NTHi strains that were associated with invasion for a given exposure. The presence/absence of genome-derived proteins between these clusters were compared to identify pathways involved in particle induced modulation of cell invasion. Based on this process, strains L267 and L341 demonstrated the largest increase in particle-induced internalization (for all exposures). While there was a significant positive correlation for NTHi without particle exposure (PC2; $p = 0.001$), the relationship was non-significant for PC1 ($p = 0.329$).

3.3.2. Protein presence associated with particle-dependent invasion

Forty-one proteins were conserved between L267 and L341 but not in the remaining isolates (Table 3). Of these, 35 were verified proteins with significant association ($p < 0.0001$). These proteins could be divided into 6 clusters based on their linkage. Cluster 1, the largest, had significant enrichment for peptide, nitrogen compound and organic substance transport (*pflA*, *frdA*, *pckA*, *nrfA*, *cydC*, *cydD*, *lysS*, *yidC*, *mnmE*, *murJ*, *tatC*, *oppA*, *sapA*, *hbpA*, *HI_1637* & *HI_1076*). These included proteins for the plasma membrane protein complex, ATP-binding cassette transporter complex, outer-membrane periplasmic space, integral component of plasma membrane and the protein containing complex. Cluster 3 had significant enrichment for oxidoreductase activity, specifically acting on NADH, quinone or similar such as ubiquinone, sodium transport, translocase or NAD (*nqrD* & *nqrC*). Cluster 5 was significant for leucine biosynthesis as well as valine, isoleucine synthesis and 2-oxocarboxylic acid metabolism (*leuC* & *leuA*). Cluster 6 was linked with the D-xylose metabolic process as well as pentose and glucuronate interconversions (*xylB* & *xylA*). Cluster 2 (*recB*, *purH* & *purF*) and cluster 4 (*abgA* & *cpdB*) had no significant functional enrichment in addition to their genetic relation.

4. Discussion

Regional Australian Indigenous communities are exposed to high levels of geogenic inorganic particulate matter (Shepherd et al., 2019), predominantly comprised of silica and iron oxide (Zosky et al., 2014). Exposure to these particles has been linked to a disproportionate burden of respiratory disease and infection (Blackall et al., 2018). However, the

Table 2

Principal component analysis (PCA) on the effects of 75 $\mu\text{g}/\text{mL}$ particle exposure on BEAS-2B cells. PC1 and PC2 cover 80% of the effects observed. Linear regression was performed on PC and invasion.

Exposure	PC1	PC2
Control	r^2 : 0.0006031 p : 0.329	r^2 : 0.2383 p : 0.001 **
Silica	r^2 : 0.3012 p : <0.001 ***	r^2 : 0.3349 p : <0.001 ***
Haematite	r^2 : 0.5228 p : <0.001 ***	r^2 : 0.7153 p : <0.001 ***
Magnetite	r^2 : 0.2406 p : 0.001 **	r^2 : 0.6486 p : <0.001 ***

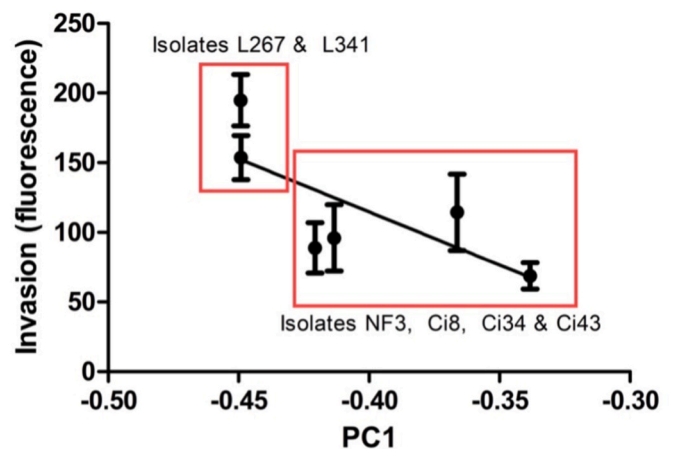


Fig. 6. An example of a monotonic association between bacterial genome similarity on the basis of principal component 1 and invasion after exposure to 75 $\mu\text{g}/\text{mL}$ of haematite for 24 h. The upper box separates isolates L267 and L341 as more invasive strains for further genomic analysis.

Table 3

Genes and associated proteins conserved within NTHi strains L267 and L341, associated with higher haematite-induced invasion.

Protein	Gene	Function
ABGA	abgA	p-aminobenzoyl-glutamate hydrolase subunit A homolog
CPDB	cpdB	2',3'-cyclic-nucleotide 2'-phosphodiesterase/3'-nucleotidase
CYDC	cydC	ATP-binding/permease protein CydC
CYDD	cydD	ATP-binding/permease protein CydD
CYOA	HI_1076	Probable cytochrome oxidase subunit 1
DDC	ddc	L-2,4-diaminobutyrate decarboxylase
FRDA	frdA	Fumarate reductase flavoprotein subunit
HBP A	hbpA	Heme-binding protein A
LEU1	leuA	2-isopropylmalate synthase
LEUC	leuC	3-isopropylmalate dehydratase large subunit
MNME	mnmE	tRNA modification GTPase MnmE
MURE	murE	UDP-N-acetylmuramoyl-L-alanyl-D-glutamate-2,6-diaminopimelate ligase
MURJ	murJ	Probable lipid II flippase MurJ
NANE	nanE	Putative N-acetylmannosamine-6-phosphate 2-epimerase
NQRC	nqrC	Na(+)-translocating NADH-quinone reductase subunit C
NQRD	nqrD	Na(+)-translocating NADH-quinone reductase subunit D
NRFA	nrfA	Cytochrome c-552
NRFE	nrfE	Cytochrome c-type biogenesis protein NrfE
OPPA	oppA	Periplasmic oligopeptide-binding protein
PCKA	pckA	Phosphoenolpyruvate carboxykinase (ATP)
PFLA	pflA	Pyruvate formate-lyase 1-activating enzyme
PRTH	prtH	Protease PrtH
PUR1	purF	Amidophosphoribosyltransferase
PUR9	purH	Bifunctional purine biosynthesis protein PurH
RECB	recB	RecBCD enzyme subunit RecB
RIBA	ribA	GTP cyclohydrolase-2
SAPA	sapA	Peptide transport periplasmic protein SapA
SYK	lysS	Lysine-tRNA ligase
TATC	tatC	Sec-independent protein translocase protein TatC
XYLA	xylA	Xylose isomerase
XYLB	xylB	Xylulose kinase
Y1005	HI_1005	Putative phosphoethanolamine transferase HI
Y1218	HI_1218	Putative L-lactate permease
Y152	HI_0152	Putative 4'-phosphopantetheinyl transferase HI
Y1637	HI_1637	Uncharacterized protein HI
Y220B	HI_220B	Uncharacterized protein HI
Y561	HI_561	Putative oligopeptide transporter HI
Y568	HI_568	Uncharacterized protein HI
Y594	HI_594	Uncharacterized protein HI
Y665	HI_665	Putative kinase HI
YIDC	YidC	Membrane protein insertase YidC

mechanism of this remains unclear. The aim of this study was to identify the impact(s) of real-world dusts and iron oxide on NTHi invasion.

Our results suggest that geogenic dusts do not increase the

invasiveness of NTHi in alveolar epithelial cells or internalization in macrophages. However, both geogenic samples induced significantly higher rates of NTHi invasion in bronchial epithelial cells when compared to control and DEP. This suggests that the mechanism of the previously documented DEP-induced increase in airway infection is not through the same as geogenic particulates. Nonetheless, in establishing that bronchial epithelial cells are more susceptible to NTHi infection, we have provided evidence towards a potential mechanism to explain epidemiological evidence linking particulate exposure with bronchiectasis, bronchitis, and upper respiratory tract infections (Blackall et al., 2018; Chang et al., 2002; Shepherd et al., 2019).

Of particular interest was the difference in effect between the Kalgoorlie and Newman dust. While both samples, which are rich in iron oxides, caused a similar response, there was some evidence to suggest that the magnitude of the response to the Newman dust (higher iron content) was greater for some NTHi strains (Zosky et al., 2014). In line with this, we saw significant increases in NTHi invasion in bronchial epithelial cells in response to haematite but not to the other primary constituent, silica. Importantly, we also tested another form of iron oxide, magnetite (Fe₃O₄), and found that the haematite effect was not replicated. This suggests that the Fe compound influences the response. Importantly, haematite is the most common form of iron in the regions where the samples were taken from and the likely the species present in these samples.

It is important to recognise that dusts from Kalgoorlie still significantly increased NTHi invasion in bronchial epithelial cells. Given the ~19% iron oxide composition of the Kalgoorlie sample (compared to 30% in Newman) (Zosky et al., 2014), this suggests that the exposure does not require large percentages of iron oxide to drastically reduce the immune defence of bronchial epithelial cells. We conducted further tests to validate the level of haematite required to induce significant NTHi uptake in bronchial epithelial cells. From this, we confirmed that concentrations as low as 25 µg/mL induced significant bacterial internalization.

Lastly, we conducted genome associations to elucidate differences in gene expression that may explain the between strain variability in the response. We identified several clusters of genes associated with elevated haematite-induced invasion. These genes were primarily associated with metabolism, particularly peptide and nitrogen metabolism and heme acquisition. Many of these genes are known to modulate virulence and are associated with host crosstalk (Baddal et al., 2015). For example, enhanced nitrogen and NADH metabolism is hypothesised to aid in mitigation of redox imbalances by NTHi, but also nitrite and nitrate that arise as part of the host defence mechanism (Othman et al., 2014). Similarly, heme acquisition has been extensively linked to NTHi virulence, and the presence of genes allowing greater heme acquisition is well correlated with increased pathogenesis (Morton et al., 2009a,b). Thus, heme acquisition gene additions such as *oppA*, *saPA*, *dppA* & *hbpA* strongly imply that NTHi isolates with higher heme acquisition will be able to establish higher levels of infection (Morton et al., 2009a,b; Morton et al., 2009a,b; Tanaka and Pinkett, 2019). Interestingly, our data suggests that these heme acquisition genes are most beneficial to bacterial invasion in the presence of iron exposure. NTHi are fastidious heme auxotrophs. This is the second line of evidence from our group that has suggested that these bacteria may be able to benefit from environmental iron (Williams et al., 2020). Combined with our functional data, it suggests that these differences in genes are not critical to haematite-induced invasion but exacerbate invasion and could be linked to more severe infection.

Our study confirmed, but also challenged, some of our previous work (Shepherd et al., 2019). In our previous study we demonstrated that geogenic particulates induced moderate levels of NTHi invasion in human airway epithelial cells (NuLi-1) (Shepherd et al., 2019) and concluded that haematite had no effect. This difference may be attributed to the particle concentration used and the cell type. Firstly, Shepherd et al. (2019) observed no effect of haematite at the 10 µg/mL

concentration (Shepherd et al., 2019). We demonstrated in our model that 10 µg/mL is below the effective level of our most sensitive cells. Previous results may have differed had 25 µg/mL of haematite, or higher, been used. Nonetheless, we demonstrated that geogenic particulates upregulated NTHi invasion, even at low concentrations. There are some limitations in our study that should be acknowledged. Whilst our data clearly outline the potential health impacts of iron-laden particulates, all studies were conducted *in vitro*. Further experiments should be carried out *in vivo* to address the limitations of *in vitro* models. Secondly, the epithelial cells used in this study were immortalised. As such, future studies should explore responses in primary cells.

This study confirms observations that geogenic particulates can increase NTHi invasion in the airway. Furthermore, we have established that the upper airway (bronchial vs alveolar) is more susceptible to particulate-induced alterations in invasion. We observed that NTHi invasion is upregulated in response to geogenic particles and that the response is likely driven by the iron content of the particles. Taken together this study presents evidence demonstrating that haematite, and geogenic particulates more broadly, can enhance respiratory bacterial infection by facilitating cell invasion. This may explain, at least in part, the higher incidence of chronic bronchitis and bronchiectasis in Indigenous Australians living in remote regions where ambient geogenic particulate levels are high. Indeed, these observations are likely to be relevant to other communities around the world where iron laden particles are in high ambient concentrations.

Author contributions

Conceptualisation, L.J.W., S.G.T. and G.R.Z.; methodology, L.J.W., S.G.T. and G.R.Z.; formal analysis, L.J.W. and G.R.Z.; investigation, L.J.W. and S.G.T.; resources, S.G.T. and G.R.Z.; data curation, L.J.W. and G.R.Z.; writing—original draft preparation, L.J.W.; writing—review and editing, S.G.T. and G.R.Z.; visualisation, L.J.W. and G.R.Z.; supervision, S.G.T. and G.R.Z.; funding acquisition, L.J.W. and G.R.Z. All authors have read and agreed to the published version of the manuscript.

Funding

This work was kindly funded by Australian Respiratory Council (Harry Windsor Grant) and Centre for Air Pollution, Energy and Health Research (PhD project grant).

Ethics approval

The study was approved by the University of Tasmania Human Research Ethics Committee (H0016505; approved on August 23, 2017).

Consent to participate

Informed consent was obtained from all subjects involved in the study.

Consent to publish

Informed consent was obtained from all subjects involved in the study.

Declaration of competing interest

The authors declare that they have no known competing financial interests or personal relationships that could have appeared to influence the work reported in this paper.

Data availability

Data will be made available on request.

Acknowledgements

This work was kindly funded by Australian Respiratory Council (Harry Windsor Grant) and Centre for Air Pollution, Energy and Health Research (PhD project grant).

References

- Altschul, S.F., Madden, T.L., Schäffer, A.A., Zhang, J., Zhang, Z., Miller, W., Lipman, D.J., 1997. Gapped BLAST and PSI-BLAST: a new generation of protein database search programs. *Nucleic Acids Res.* 25 (17), 3389–3402. <https://doi.org/10.1093/nar/25.17.3389>.
- Angrill, J., Agustí, C., de Celis, R., Rañó, A., Gonzalez, J., Solé, T., Xaubet, A., Rodriguez-Roisin, R., Torres, A., 2002. Bacterial colonisation in patients with bronchiectasis: microbiological pattern and risk factors. *Thorax* 57 (1), 15. <https://doi.org/10.1136/thorax.57.1.15>.
- Australian Bureau of Statistics, 2017. *Aboriginal and Torres Strait Islander Peoples: Smoking Trends, Australia*. ABS, Canberra, p. 1994 to 2014-15.
- Baddal, B., Muzzi, A., Censini, S., Calogero, R.A., Torricelli, G., Guidotti, S., Taddei, A.R., Covacci, A., Pizzi, M., Rappuoli, R., Soriani, M., Pezzicoli, A., 2015. Dual RNA-seq of nontypeable *Haemophilus influenzae* and host cell transcripts reveals novel insights into host-pathogen cross talk. *mBio* 6 (6). <https://doi.org/10.1128/mBio.01765-15>, 01765-01715.
- Bankevich, A., Nurk, S., Antipov, D., Gurevich, A.A., Dvorkin, M., Kulikov, A.S., Lesin, V. M., Nikolenko, S.I., Pham, S., Pribelski, A.D., Pyshkin, A.V., Sirotkin, A.V., Vyahhi, N., Tesler, G., Alekseyev, M.A., Pevzner, P.A., 2012. SPAdes: a new genome assembly algorithm and its applications to single-cell sequencing. *J. Comput. Biol.* 19 (5), 455–477. <https://doi.org/10.1089/cmb.2012.0021>.
- Blackall, S.R., Hong, J.B., King, P., Wong, C., Einsiedel, L., Remond, M.G.W., Woods, C., Maguire, G.P., 2018. Bronchiectasis in indigenous and non-indigenous residents of Australia and New Zealand. *Respirology* 23 (8), 743–749. <https://doi.org/10.1111/resp.13280>.
- Bolger, A.M., Lohse, M., Usadel, B., 2014. Trimmomatic: a flexible trimmer for Illumina sequence data. *Bioinformatics* 30 (15), 2114–2120. <https://doi.org/10.1093/bioinformatics/btu170>.
- Bradbury, R., Champion, A., Reid, D.W., 2008. Poor clinical outcomes associated with a multi-drug resistant clonal strain of *Pseudomonas aeruginosa* in the Tasmanian cystic fibrosis population. *Respirology* 13 (6), 886–892. <https://doi.org/10.1111/j.1440-1843.2008.01383.x>.
- Bradbury, R.S., Champion, A.C., Reid, D.W., 2009. Epidemiology of *Pseudomonas aeruginosa* in a tertiary referral teaching hospital. *J. Hosp. Infect.* 73 (2), 151–156. <https://doi.org/10.1016/j.jhin.2009.05.021>.
- Camacho, C., Coulouris, G., Avagyan, V., Ma, N., Papadopoulos, J., Bealer, K., Madden, T.L., 2009. BLAST+: architecture and applications. *BMC Bioinform.* 10 (1), 421. <https://doi.org/10.1186/1471-2105-10-421>.
- Castranova, V., Ma, J.Y., Yang, H.M., Antonini, J.M., Butterworth, L., Barger, M.W., Roberts, J., Ma, J.K., 2001. Effect of exposure to diesel exhaust particles on the susceptibility of the lung to infection. *Environ. Health Perspect.* 109 (4), 609–612. <https://doi.org/10.1289/ehp.01109s4609>.
- Chang, A.B., Grimwood, K., Mulholland, E.K., Torzillo, P.J., 2002. Bronchiectasis in indigenous children in remote Australian communities. *Med. J. Aust.* 177 (4), 200–204.
- Chikaura, H., Nakashima, Y., Fujiwara, Y., Komohara, Y., Takeya, M., Nakanishi, Y., 2016. Effect of particle size on biological response by human monocyte-derived macrophages. *Biosurface and Biotechnology* 2 (1), 18–25. <https://doi.org/10.1016/j.bsbt.2016.02.003>.
- Clementi, C.F., Murphy, T.F., 2011. Non-typeable *Haemophilus influenzae* invasion and persistence in the human respiratory tract. *Front. Cell. Infect. Microbiol.* 1 <https://doi.org/10.3389/fcimb.2011.00001>, 1-1.
- Clifford, H., Pearson, G., Franklin, P., Walker, R., Zosky, G., 2015. Environmental health challenges in remote Aboriginal Australian communities: clean air, clean water and safe housing. *Aust. Indig. Health Bull.* 15, 1–13.
- Esen, M., Grassmé, H., Riethmüller, J., Riehle, A., Fassbender, K., Gulbins, E., 2001. Invasion of human epithelial cells by *Pseudomonas aeruginosa* involves src-like tyrosine kinases p60Src and p59Fyn. *Infect. Immun.* 69 (1), 281–287. <https://doi.org/10.1128/IAI.69.1.281-287.2001>.
- Foxwell, A.R., Kyd, J.M., Cripps, A.W., 1998. Nontypeable *haemophilus influenzae*: pathogenesis and prevention. *Microbiol. Mol. Biol. Rev.* 62 (2), 294–308.
- Government of South Australia, 2007. *Whyalla Health Impact Study Report*. Adelaide, South Australia.
- Government of Western Australia, 2016. *Port Hedland Air Quality Health Risk Assessment for Particulate Matter*.
- Gurevich, A., Saveliev, V., Vyahhi, N., Tesler, G., 2013. QUAST: quality assessment tool for genome assemblies. *Bioinformatics* 29 (8), 1072–1075. <https://doi.org/10.1093/bioinformatics/btt086>.
- Ljung, K., Siah, W.S., Devine, B., Maley, F., Wensinger, A., Cook, A., Smirk, M., 2011. Extracting dust from soil: improved efficiency of a previously published process. *Sci. Total Environ.* 410–411, 269–270. <https://doi.org/10.1016/j.scitotenv.2011.07.061>.
- Melody, S.M., Bennett, E., Clifford, H.D., Johnston, F.H., Shepherd, C.C.J., Alach, Z., Lester, M., Wood, L.J., Franklin, P., Zosky, G.R., 2016. A cross-sectional survey of environmental health in remote Aboriginal communities in Western Australia. *Int. J. Environ. Health Res.* 26 (5–6), 525–535. <https://doi.org/10.1080/09603123.2016.1194384>.
- Morton, D.J., Seale, T.W., Bakaletz, L.O., Jurcisek, J.A., Smith, A., VanWagoner, T.M., Whitby, P.W., Stull, T.L., 2009a. The heme-binding protein (HbpA) of *Haemophilus influenzae* as a virulence determinant. *Int. J. Med. Microbiol.* 299 (7), 479–488. <https://doi.org/10.1016/j.ijmm.2009.03.004>.
- Morton, D.J., Seale, T.W., VanWagoner, T.M., Whitby, P.W., Stull, T.L., 2009b. The dppBCDF gene cluster of *Haemophilus influenzae*: role in heme utilization. *BMC Res. Notes* 2, 166. <https://doi.org/10.1186/1756-0500-2-166>.
- Mullan, N., Codde, J., Van Buynder, P., 2006. *Respiratory Hospitalisations in Port Hedland, 1993-2004: an Exploratory Geographical Analysis*.
- O'Grady, K.A., Torzillo, P.J., Chang, A.B., 2010. Hospitalisation of Indigenous children in the Northern Territory for lower respiratory illness in the first year of life. *Med. J. Aust.* 192 (10), 586–590. <https://doi.org/10.5694/j.1326-5377.2010.tb03643.x>.
- Othman, D.S., Schirra, H., McEwan, A.G., Kappler, U., 2014. Metabolic versatility in *Haemophilus influenzae*: a metabolomic and genomic analysis. *Front. Microbiol.* 5, 69. <https://doi.org/10.3389/fmicb.2014.00069>.
- Page, A.J., Cummins, C.A., Hunt, M., Wong, V.K., Reuter, S., Holden, M.T.G., Fookes, M., Falush, D., Keane, J.A., Parkhill, J., 2015. Roary: rapid large-scale prokaryote pan genome analysis. *Bioinformatics* 31 (22), 3691–3693. <https://doi.org/10.1093/bioinformatics/btv421>.
- Pak, A., Adegboye, O.A., Eisen, D.P., McBryde, E.S., 2021. Hospitalisations related to lower respiratory tract infections in Northern Queensland. *Australian and New Zealand Journal of Public Health* 45 (5), 430–436.
- Pinto, E.H., Longo, P.L., Camargo, C.C. B.d., Dal Corso, S., Lanza, F.D.C., Stelmach, R., Athanazio, R., Fernandes, K.P.S., Mayer, M.P.A., Bussadori, S.K., Mesquita Ferrari, R. A., Horliana, A.C.R.T., 2016. Assessment of the quantity of microorganisms associated with bronchiectasis in saliva, sputum and nasal lavage after periodontal treatment: a study protocol of a randomised controlled trial. *BMJ Open* 6 (4), e010564. <https://doi.org/10.1136/bmjopen-2015-010564>.
- Pizzutto, S.J., Hare, K.M., Upham, J.W., 2017. Bronchiectasis in children: current concepts in immunology and microbiology. *Frontiers Pediatr.* 5 (123) <https://doi.org/10.3389/fped.2017.00123> [Review].
- Rubins, J.B., 2003. Alveolar macrophages. *Am. J. Respir. Crit. Care Med.* 167 (2), 103–104. <https://doi.org/10.1164/rccm.2210007>.
- Seemann, T., 2014. Prokka: rapid prokaryotic genome annotation. *Bioinformatics* 30 (14), 2068–2069. <https://doi.org/10.1093/bioinformatics/btu153>.
- Shepherd, C.C.J., Clifford, H.D., Mitrou, F., Melody, S.M., Bennett, E.J., Johnston, F.H., Knibbs, L.D., Pereira, G., Pickering, J.L., Teo, T.H., Kirkham, L.S., Thornton, R.B., Kicic, A., Ling, K.M., Alach, Z., Lester, M., Franklin, P., Reid, D., Zosky, G.R., 2019. The contribution of geogenic particulate matter to lung disease in indigenous children. *Int. J. Environ. Res. Publ. Health* 16 (15). <https://doi.org/10.3390/ijerph16152636>.
- Siegel, P.D., Saxena, R.K., Saxena, Q.B., Ma, J.K.H., Ma, J.Y.C., Yin, X.-J., Castranova, V., Al-Humaidi, N., Lewis, D.M., 2004. Effect of diesel exhaust particulate (DEP) on immune responses: contributions of particulate versus organic soluble components. *J. Toxicol. Environ. Health, Part A* 67 (3), 221–231. <https://doi.org/10.1080/15287390490266891>.
- Szklarczyk, D., Gable, A.L., Lyon, D., Junge, A., Wyder, S., Huerta-Cepas, J., Simonovic, M., Doncheva, N.T., Morris, J.H., Bork, P., Jensen, L.J., Mering, C.V., 2019. STRING v11: protein-protein association networks with increased coverage, supporting functional discovery in genome-wide experimental datasets. *Nucleic Acids Res.* 47 (D1), D607–d613. <https://doi.org/10.1093/nar/gky1131>.
- Tanaka, K.J., Pinkett, H.W., 2019. Oligopeptide-binding protein from nontypeable *Haemophilus influenzae* has ligand-specific sites to accommodate peptides and heme in the binding pocket. *J. Biol. Chem.* 294 (3), 1070–1082. <https://doi.org/10.1074/jbc.RA118.004479>.
- Watson, K., Carville, K., Bowman, J., Jacoby, P., Riley, T.V., Leach, A.J., Lehmann, D., 2006. Upper respiratory tract bacterial carriage in Aboriginal and non-Aboriginal children in a semi-arid area of Western Australia. *Pediatr. Infect. Dis. J.* 25 (9), 782–790. <https://doi.org/10.1097/01.inf.0000232705.49634.68>.
- Williams, L.J., Tristram, S.G., Zosky, G.R., 2020. Inorganic particulate matter modulates non-typeable *Haemophilus influenzae* growth: a link between chronic bacterial infection and geogenic particles. *Environ. Geochem. Health* 42 (7), 2137–2145. <https://doi.org/10.1007/s10653-019-00492-3>.
- Witherden, E.A., Tristram, S.G., 2013. Prevalence and mechanisms of beta-lactam resistance in *Haemophilus haemolyticus*. *J. Antimicrob. Chemother.* 68 (5), 1049–1053. <https://doi.org/10.1093/jac/dks532>.
- Yang, H.M., Antonini, J.M., Barger, M.W., Butterworth, L., Roberts, B.R., Ma, J.K., Castranova, V., Ma, J.Y., 2001. Diesel exhaust particles suppress macrophage function and slow the pulmonary clearance of *Listeria monocytogenes* in rats. *Environ. Health Perspect.* 109 (5), 515–521. <https://doi.org/10.1289/ehp.01109s515>.
- Zosky, G.R., Iosifidis, T., Perks, K., Ditcham, W.G.F., Devadason, S.G., Siah, W.S., Devine, B., Maley, F., Cook, A., 2014. The concentration of iron in real-world geogenic pm10 is associated with increased inflammation and deficits in lung function in mice. *PLoS One* 9 (2), e90609. <https://doi.org/10.1371/journal.pone.0090609>.